



Supporting Online Material for

Phosphorylation Networks Regulating JNK Activity in Diverse Genetic Backgrounds

Chris Bakal,* Rune Linding, Flora Llense, Elleard Heffern, Enrique Martin-Blanco, Tony Pawson, Norbert Perrimon

*To whom correspondence should be addressed. E-mail:
cbakal@receptor.med.harvard.edu

Published 17 October 2008, *Science* **322**, 453 (2008)
DOI: 10.1126/science.1158739

This PDF file includes

Materials and Methods
SOM Text
Figs. S1 and S2

Materials and Methods

Protocols

Description of the dJUN-FRET reporter: A reporter for JNK-mediated phosphorylation was constructed analogously to a previously described reporter for Protein Kinase C (PKC) (1). This reporter, dJUN-FRET, was composed of monomeric CFP (mCFP) and monomeric YFP (mYFP) flanking a JNK substrate sequence tethered by a flexible linker to a FHA2 phosphothreonine-binding domain from the yeast checkpoint protein Rad53p. Phosphorylation of the substrate sequence triggers an intramolecular clamp with the FHA2 module causing a conformational change that alters the amount of FRET from CFP to YFP. Thus dJUN-FRET provides continuous non-destructive fluorometric readout for JNK activity. In designing these constructs, we used FHA2 as it is monomeric and has a modest affinity for phospho-threonine making the sensor reversible and thereby enabling monitoring of the ongoing balance between kinases and phosphatases. We designed a specific JNK substrate sequence that would bind FHA2. This sequence was designed *de novo* based on the phosphorylation site of JUN (2), the best-characterized target of JNK where the reactive serine residues from the phosphorylation site was substituted by threonines: GGSGGLLPDVGLLKLAtPEGGSGG (JUN). The underlined region represented the substrate sequence, flanked by a flexible GGSGG linker. We placed the dJUN-FRET reporter under the control of a constitutive *actin* promoter for expression in *Drosophila* cells in culture.

FRET sensor cloning: In order to build the dJUN-FRET sensor, we fused an FHA2 phosphothreonine binding domain and a JUN fragment containing the JNK phosphorylation site. The FHA2 domain came from the CKAR vector (1). To clone this fragment, we used the following primers:

5' CCG TCG ACT TTT TAA CTT TAA AAC CAT TGC 3'

and

5' CGT TAA TTT CCA CTT TAA AGG ATCC 3'.

The CKAR plasmid was subjected to PCR following standard procedures. The annealing temperature was 65°C for 30 cycles. The resulting amplified fragment was 378 base pairs. The JUN domain was generated by annealing of two primers that introduce a serine to threonine substitution at the critical phosphorylation site and containing appropriate enzyme restriction sites for cloning. The two primers are:

5' GA TCC GGA GGC AGC GGA GGT CTT CTC ACG

ACG CCC GAC GTC GGG CTG C TC AAG CTG GCG ACG CCG GAG GGA GGC AGC GGC 3'

and

5'GGC CGC CGC GCT GCC TCC CTC CGG CGT CGC CAG CTT GAG CCC GAC GTC GGG CGT
CGT GAG AAG ACC TCC GCT GCC TCG G 3'.

This fragment was subcloned into a FRET vector (Raichu-Ras X46) (3) containing YFP and CFP. A fragment containing YFP-FHA2-linker-JUN domain-CFP was then subcloned into the ACT5 vector.

Monitoring the dJUN-FRET activity: The simplest way to measure FRET is to evaluate the ratio of the mean YFP/CFP intensity after CFP excitation. The emission signal of the FRET sensors at the CFP excitation maximum (434 nm) before and after phosphorylation by JNK can be detected by confocal microscopy, or microscopes equipped with EM-CCD cameras and specific filters for detection of CFP (480nm) and YFP (525nm).

Cell culturing and transfections: *Drosophila* BG-2 cells were cultured in Shields and Sang M3 insect media (Sigma), 10% Fetal Bovine Serum (Sigma), 10 µg/ml Insulin (Sigma), and Penicillin-Streptomycin (Gibco). Each screen was performed by first transfecting BG-2 cells with *actin*-dJUN-FRET 2-3 days prior to transfecting the cells again with dsRNAs. Both DNA and dsRNA transfections were performed using Effectene transfection reagent (Qiagen). Cells were transfected as described in detail at <http://www.flyrnai.org>. Whereas we observed 10-30% transfection efficiency of the dJUN-FRET reporter, we consistently observed that dsRNAs elicited expected control phenotypes (such as cell death caused by *thread* dsRNA, or binucleation caused by *RacGAP50C/MgcRacGAP* dsRNA) in nearly all cells.

We transfected BG-2 cells with dsRNAs in a 384-well format. The Kinase-Phosphatase (KP) mini-library is a normalized dsRNA library, and each well contains 0.25 µg of dsRNA targeting a single gene. For combinatorial experiments we added a second dsRNA to the cells in suspension prior to plating. The second dsRNA was diluted such that cells in each well were incubated with an additional 0.25 µg of dsRNA. Four days following dsRNA transfection, we imaged live cells.

Design of mini RNAi library targeting *Drosophila* Kinases and Phosphatases: The total KP mini-library contains 1395 dsRNAs, not including controls, plated on eight 384-well plates (DRSC IDs 401-408). The dsRNAs have been designed to have zero, or extremely few off-target effects (OTEs). Supplemental Table 1 lists every dsRNA used in our screens and the number of predicted OTEs. Description of the OTE prediction algorithms is described at www.flyrnai.org.

In the KP screen, we screened all 8 plates that comprised the collection. However in the 12 combinatorial screens described in this study, we screened only the first 7 plates of the collection (401-407) containing 1,477 total dsRNAs, which includes 156 *lacZ* dsRNAs, and 1,321 gene specific dsRNAs targeting a total of 482 genes with 2-9 independent dsRNAs. Only multiple dsRNAs targeting 4 genes, *cdc14* (PPase), *CG34356* (kinase), *CG34384* (kinase), *CG34455*, are not tested in any screen by excluding Plate 408. Thus in each of the 12 screens 1,477 dsRNAs are tested in combination with a query dsRNA totaling 17,724 individual combinatorial tests.

High-throughput automated image analysis: In order to calculate the effects of individual dsRNAs on dJUN-FRET activity in a high-throughput manner, we imaged cells using the Evotec Opera Microscope using a 40X water immersed objective. Due to the stochastic nature of dJUN-FRET transfection it was necessary to image 35 sites per well in order to image, segment, and measure significant numbers of dJUN-FRET transfected cells per well (50-200). Each field typically contained 0-3 cells. Since BG-2 cells are highly motile, transfected cells were rarely observed to be in contact with one another thereby facilitating cell segmentation.

Following imaging, we implemented the following automated protocol (Seungtaek Lee, Perkin Elmer) in order to quantify a dJUN-FRET ratio per well:

1. Individual cell detection.
 - a. Use the YFP signal (present in all cells) to identify individual cells
 - b. Use the YFP signal to accurately detect cell edges to get accurate cell area
2. Calculate mean YFP signal intensity (individual pixel intensity can range from 0 to 4095) in the entire cell area for each cell.
3. Calculate mean CPF signal intensity in the entire cell area (same area as in step 2) for each cell.
4. Calculate the ratio of YFP to CFP intensity (YFP_intensity/CFP_intensity) for each cell.
5. Calculate the area (in pixels) of each cell.
6. Steps 1 through 5 are repeated for each field.
7. Export the following data for each cell (for all the cells in all the fields):
 - a. Cell area
 - b. Mean YFP intensity
 - c. Mean CFP intensity
 - d. YFP-CFP ratio

Data Normalization: Each screen was performed in duplicate, or in some cases quadruplicate, and a normalized FRET:CFP ratio for each well/dsRNA was devised by calculating a weighted mean FRET:CFP ratio for replicate wells based on the number of cells scored in each well.

$$\frac{(\text{RATIO A1_REP1} \times \text{Cell Number A1_REP1}) + (\text{RATIO A1_REP2} \times \text{Cell Number A1_REP2})}{\text{Cell Number A1_REP1} + \text{Cell Number A1_REP2}}$$

Each weighted FRET:CFP ratio is then normalized by expressing the well ratio as a percentage of the mean ratio of all wells across replicate plates. A Z-score is then calculated by subtracting the mean FRET score for all empty/control wells (e.g. *lacZ* dsRNA containing wells) across all screens and dividing the difference by the standard deviation of the empty/control well population. Z is the distance between the weighted mean sample score and the control mean in units of the standard deviation. Z is negative when the raw score is below the mean, positive when above.

Testing of other genes as JNK regulators

During the course of these studies we tested a number of additional dsRNAs that were not in the KP set for the ability to up- or down-regulate dJUN-FRET reporter activity in BG-2 cells (Supplemental Table 1 and Supplemental Figure 1). Specifically, we tested a number of genes involved in Rho signaling as Rho GTPases have been extensively implicated as upstream activators of JNK signaling (4-6).

Gene	dsRNAs Tested (DRSC ID)	Predicted Off-targets
<i>Rac1</i>	DRSC25131	0
<i>Rho1</i>	DRSC07530	0
<i>Cdc42</i>	DRSC25134	0
<i>CdGAPr</i>	DRSC02389	0
<i>p190RhoGAP</i>	DRSC20097	0
<i>sif/still-life</i>	DRSC11395	0
<i>RacGAP50C/MgcRacGAP/tumbleweed</i>	DRSC07575	0
<i>RhoGEF2</i>	DRSC07531	1
<i>pbl/pebble</i>	DRSC11381	3
<i>Mtl</i>	DRSC16751	0

Table 1: List of dsRNAs used to test Rho components as regulators of JNK Signaling. The Drosophila RNAi Screening Center (DRSC) IDs of dsRNAs used to inhibit Rho components in this study and the number of predicted Off-targets for each dsRNA are shown.

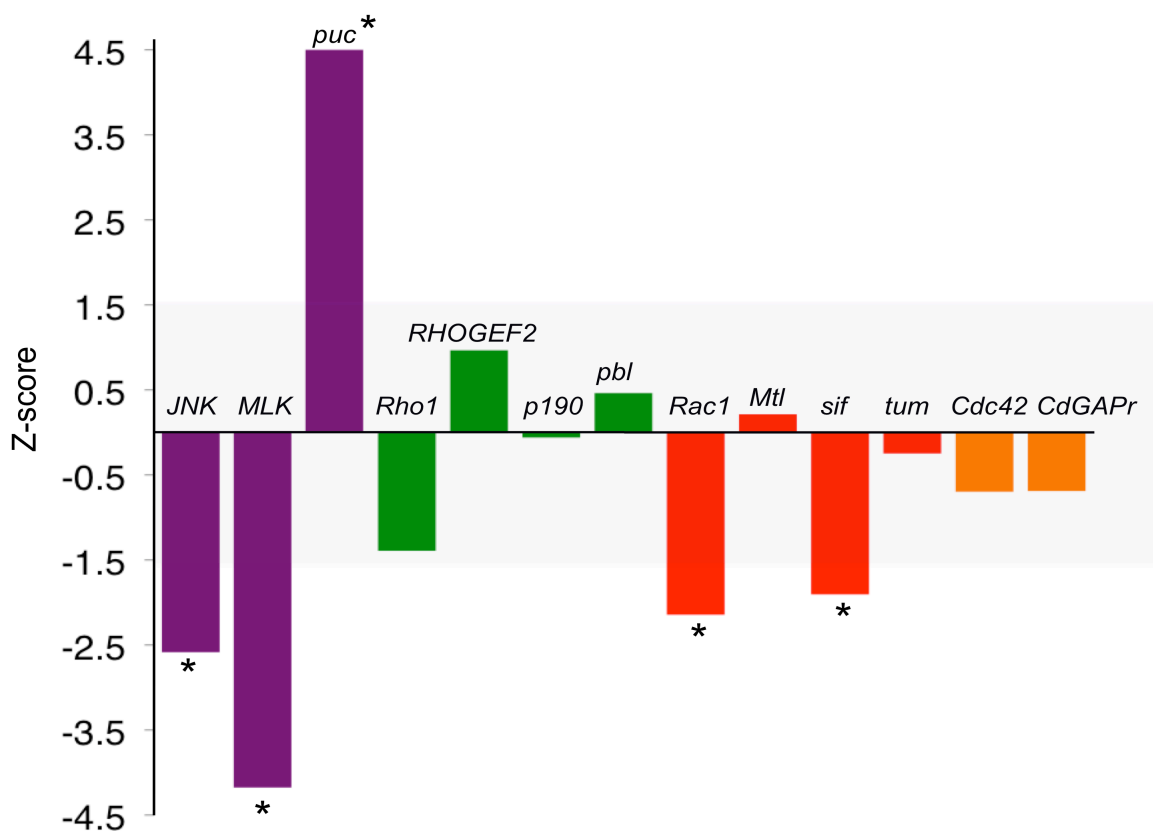


Figure 1. Effect of dsRNA-mediated inhibition of Rho components on dJUN-FRET activity. Z-score threshold for significance is set at $Z = \pm 1.5$, and asterisk indicates dsRNAs (described in Supplemental Table 1) that produced a significant change in dJUN-FRET reporter activity versus control dsRNAs.

We also tested whether inhibition of the tumor-suppressor gene *VHL* (7) affected JNK signaling directly, as we aimed to use this as a query gene in combinatorial RNAi screens. However, targeting *VHL* by DRSC07716 did not significantly up- or down- regulate dJUN-FRET reporter activity.

Sensitized Screens

Identifying JNK regulators in each screen: In each screen, individual genes are scored as JNK regulators if transfection with two independent dsRNAs resulted in a mean Z-score above/below a pre-determined threshold. For the KP screen the threshold was fixed at a Z-score of ± 2.0 . Due to the fact that the distributions of Z-scores for individual sensitized screens had diverse shapes (e.g. differing heights or were partially skewed), meaning some dsRNAs clearly affected the sensitivity of the dJUN-FRET reporter (Fig. 2), we chose the 0.05 and 0.95 percentile for each combinatorial screen as a threshold score (Supplemental Methods Table 2). The only exception was that the threshold for *MLK/slpr* suppressors was lowered to include *ERK/rl* and *msn* dsRNAs, which on the basis of the KP screens were considered positive controls for JNK enhancers.

Screen	Z-score threshold for Enhancers (0.05 percentile)	Z-score threshold for Suppressors (0.95 percentile)
KP/Rac1	-2.09	1.67
KP/Cdc42	-5.57	1.34
KP/rl (ERK)	-2.40	1.67
KP/AKT	-3.06	2.21
KP/PTEN	-2.10	1.74
KP/Sif	-1.619	1.14
KP/p190RhoGAP	-1.66	1.37
KP/VHL	-5.67	6.09
KP/puc	-2.72	3.07
KP/slpr (MLK)	-1.89	3.70 (*2.60)
KP/bsk (JNK)	-2.01	1.88
KP/hippo	-1.68	1.58

Table 2. Z-score thresholds used to identify JNK enhancers and suppressors. Asterisk indicates that in the case of KP/slpr suppressors a lowered Z-score was used such that *rl* and *msn* mean Z-scores passed the threshold.

Isolating genes as high-confidence JNK regulators across multiple combinatorial screens:

We observed that individual genes were identified as JNK regulators across multiple screens with varying frequency. For example *CycA* was identified as a JNK regulator in 7 of 12 screens, whereas *Fak65D* was identified in a single screen. In order to determine a significance threshold for the likelihood of genes being isolated as hits across screens, we calculated the probability of a gene being identified as a hit in terms of the number of dsRNAs targeting that gene in the KP set (Supplemental Figure 2). The majority of genes are targeted by 2-4 dsRNAs, and the probability

of these genes being identified as hits in 2 out of 11 screens is $P < 0.001^{**}$. Thus genes targeted by 2-4 dsRNAs are considered high-confidence JNK regulators if the gene is identified as a hit in ≥ 2 screens (Supplemental Table 3). Genes targeted by 5-7 dsRNAs are considered high-confidence JNK regulators only if scored as hits in ≥ 3 screens (Supplemental Table 3). Lastly, *Mod9(mgd)*, targeted by 9 dsRNAs is also considered a high-confidence JNK regulator as it was identified as a hit in 4 different combinatorial screens.

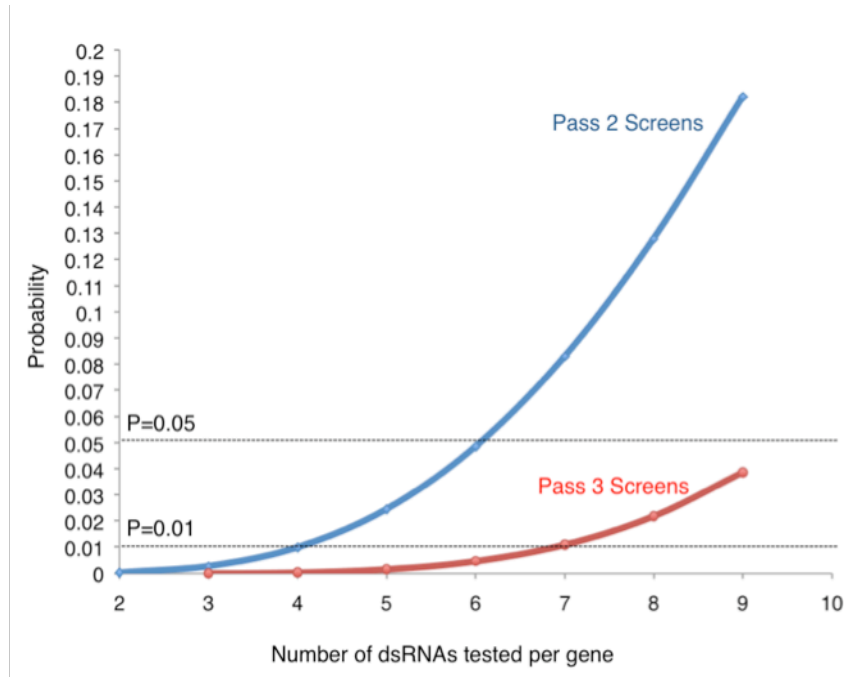


Figure 2. Determining a significance threshold for JNK regulators across RNAi Screens. The probability of a gene being identified as a hit in 2/11 (blue line) or 3/11 (red line) screens was calculated as a function of the number of dsRNAs targeting that gene the KP set.

* We based these calculations on 11 screens as the 12th screen involving *Hippo* dsRNA was performed after this statistical analysis. However, this does not affect the outcome of this analysis.

Validation of JNK Regulators

Quantitative Real-time PCR: BG-2 cells were transfected with dsRNAs targeting candidate genes (Supplemental Table 3) and five days later (unless otherwise indicated) total RNA was prepared using Trizol reagent (Invitrogen) as suggested by the manufacturer. cDNA was then prepared from ~1 µg of total RNA using Qiagen QuantiTect Reverse Transcription kit. Quantitative Real-time PCR was then performed using the Qiagen QuantiTect SYBR Green RT-PCR kit.

Gene	dsRNAs Tested (DRSC ID)	Predicted Off-targets
<i>bsk/JNK</i>	DRSC36595	0
<i>slpr/MLK</i>	DRSC36809	0
<i>puc</i>	DRSC36627	0
<i>otk</i>	DRSC07658	1
<i>ial</i>	DRSC23324	0
<i>sgg/GSK</i>	DRSC17228	1
<i>ptp99a</i>	DRSC22125	0
<i>rl/ERK</i>	DRSC21814	0
<i>ERK7</i>	DRSC21895	0
<i>ckI alpha</i>	DRSC23308	0
<i>dlg1</i>	DRSC36997	0
<i>warts</i>	DRSC25766	0

Table 3: List of dsRNAs used to test candidate genes as regulators of *MMP1* RNA levels

The following primer pairs were used in RT-PCR Experiments

MMP1:

5' ACGACTCCATCTGCAAGGAC 3'

and

5' GGAGATGAGCTGTGGGTA 3'

PKA:

5' CAATCAGCAGATTCTCCGGCT 3'

and

5' AGCCGCACTCGCGCTTCTAC 3'

puckered:

5' TTT CTG CTG ACT RGC CAC AC 3'

and

5' TAG CAT TCG CGT TAC ACT GC 3'

In each sample *MMP1* and *puckered* levels were compared to levels of *PKA*. *MMP1/Pka* or *pac/PKA* ratios were then normalized to control-transfected cells. Each sample was minimally run in quadruplicate. Tests for significant differences ($P < 0.01$) were performed using Student's T-test.

JNK Phosphorylation Network Construction

We obtained a mass-spectrometry based phospho-proteome measured in *Drosophila* Kc167 cells (8). This set consisted of 10,118 high-confidence phosphorylation sites from 3472 gene models and 4583 distinct phospho-proteins. These data served as input for NetworKIN version 2.0b (<http://networkin.info>) (9, 10), which is powered by the NetPhorest motif engine (11). We used a cutoff of 0.7 on the NetworKIN ranking score; this corresponds to a requirement of any given kinase group member to be within 70% of the top-scoring kinase for a particular site. Within a kinase group we used a cutoff of 0.95 to determine a specific kinase for the site, this corresponds to a requirement of any given gene specific kinase to be within 95% of the top-scoring kinase for the site. The predictions were subsequently filtered to only contain either kinases or substrates that were identified by the RNAi screens.

The resulting high-confidence site-specific network was extended with predictions for ERK kinase (Rolled/Rl kinase). Due to a weaker contextual network for this kinase, these predictions were obtained with a lower cutoff of 0.4 on the ranking score. The final JNK phosphorylation network (attached as *submission_.70_rl_.40.txt*) spanned 78 phosphorylation sites on 20 proteins and 120 edges between 20 substrates and 7 kinases. In order to reduce this to a directional interaction network we assigned each edge an interaction strength corresponding to the average NetworKIN ranking score for all the sites linking a kinase to a substrate. This resulted in a linear interaction strength scale for the edges visualized on Supplemental Figure 3. The visualization was performed using Cytoscape-2.3.5 (12) and the hierarchical layout algorithm from the “y-files” plugin. Finally the network layout was hand-edited to optimize its visualization.

JNK Phosphorylation Network Topology Analysis

We analyzed the JNK network as a directional protein-protein interaction network with kinases pointing at substrates. We subjected this network (Supplemental Figure 3) to topological analysis as described in (9). Briefly, we used Cytoscape-2.3.5 (12) with the NetworkAnalyzer plugin (<http://med.bioinf.mpi-inf.mpg.de/netanalyzer/index.php>) to calculate the topological parameters of the network. The result of this analysis is attached in Supplemental Table S5. In particular we noted increased betweenness-centrality for specific nodes in the network. We also note that the network resembles an hourglass and is scale-free according to fitting of the degree distribution of the corresponding undirected network.

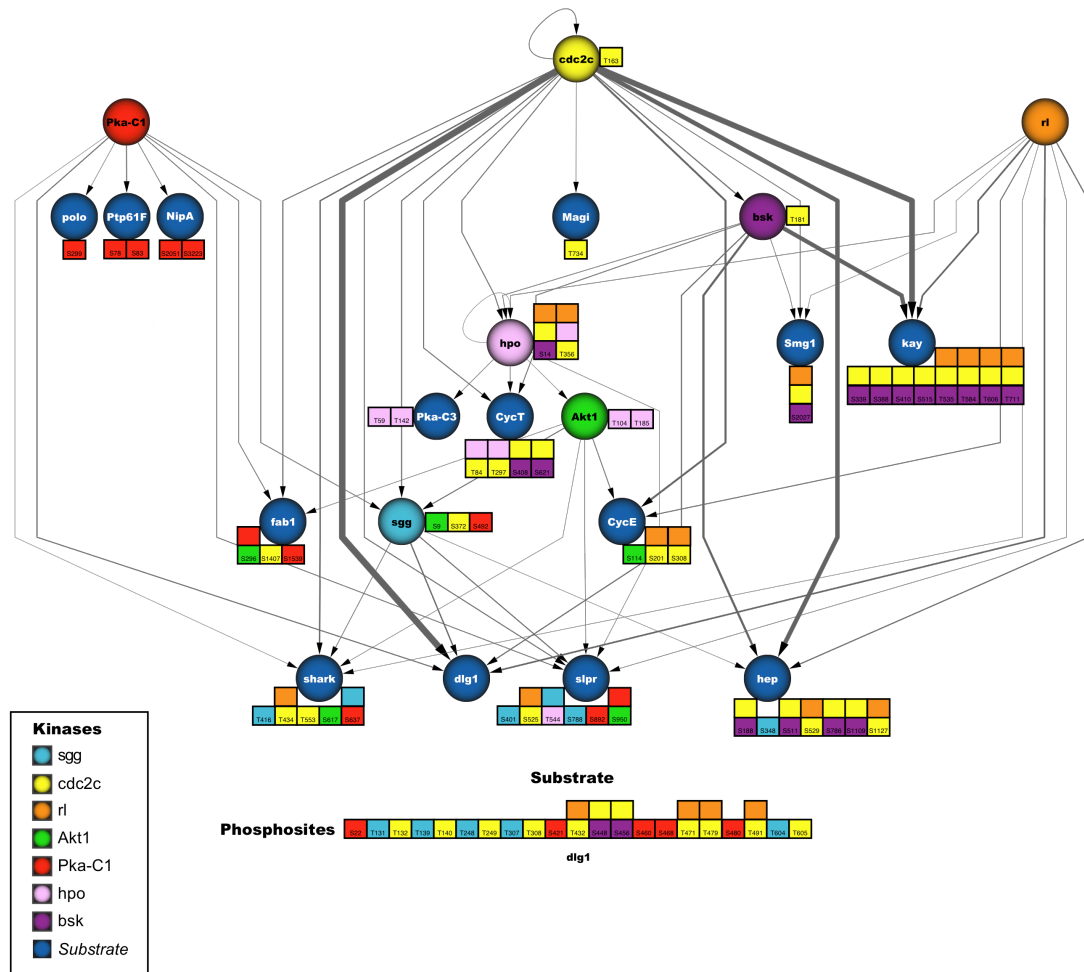


Figure 3. Computational Reconstruction of the JNK phosphorylation network by the NetworkKIN algorithm. (A) We used the NetworkKIN algorithm and a recent *Drosophila* phosphoproteome (8) to derive a directional network of potential kinase-substrate relationships amongst JNK regulators identified by RNAi screening. The edges between the nodes correspond to predictions from NetworkKIN and their width correspond to the interaction strength (Supplemental Material, <http://genepath.med.harvard.edu/~cbakal/Supplemental>). For example, there are strong predicted interactions (based on several phosphorylation sites) between *cdc2c*/CDK2 and Dlg1 as well as *bsk*/JNK and *kay*/FOS. Protein kinases we could perform target prediction for using NetworkKIN are shown in various colors and the corresponding phosphorylation sites are indicated with similarly colored boxes (using Dlg1 as example) on the corresponding targets. Protein kinases not currently covered by NetworkKIN or non-kinases are shown in blue. Phosphorylation sites NetworkKIN predicts to be targeted by more than one kinase are shown as stacked boxes. The position of proteins within the network is hierarchical based on the networks directionality (kinases pointing towards substrates) as reflected number of out- and in-bound interactions.

Supplemental Text

Here we discuss in detail additional findings of our study regarding the role of JNK in cell-cycle progression.

Genes involved in cell-cycle entry or G2-M progression (e.g. *CDK4*, *CDK2*, *CycA*, *CycE*), or spindle checkpoint signaling (*Tao-1* (13)) were isolated as JNK suppressors whereas regulators of spindle assembly and cytokinesis (e.g. *polo*, *ial*, *Nipped-A*, *Pp1-87B*) scored as JNK enhancers. These data suggest that JNK activity is actively downregulated during the G1 to M phases of the cell cycle, but is increased during late mitosis and cytokinesis (14-18). In support of the notion that JNK is largely downregulated by cell cycle entry and proliferative signaling, we identified *ERK* as a JNK suppressor in the KP screen, and subsequently identified *KSR* and *RAF* in sensitized screens (Fig. 3). These findings are consistent with *in vivo* studies demonstrating that strong ERK signaling serves to repress JNK-mediated apoptosis (19). *ERK*, *CDK2*, *CycA*, and *puc* dsRNA have correlated scores consistent across screens suggesting that *puc* is a transcriptional target of both ERK (fig. s1) and CDK2 activity (Fig. 4). Cross talk also occurs between ERK and JNK pathways upstream of JNK itself, as illustrated by the fact that in a background of *puc* deficiency we detect *ERK* as an activator of JNK (Fig. 4), and predict JNKK and MLK as ERK substrates (Fig. 3). We propose a two-mode model of Fos regulation. JNK and CDK2 activate FOS via phosphorylation of the same residues, but JNK does so in interphase or response to stress as (20), while CDK2 targets these sites during cell-cycle progression (Supplemental Figure 4).

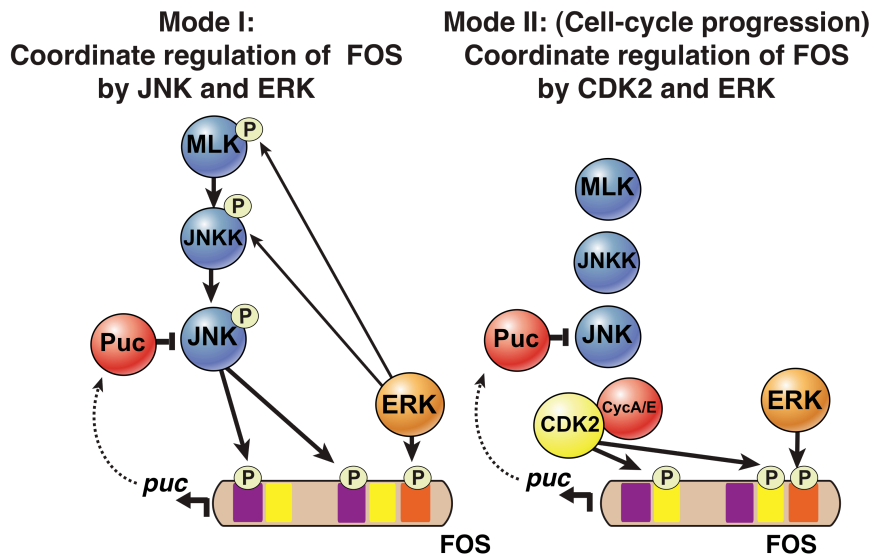


Figure 4. Two-mode Model of FOS Regulation by JNK/ERK and CDK2/ERK.

References

1. J. D. Violin, J. Zhang, R. Y. Tsien, A. C. Newton, *J Cell Biol* **161**, 899 (Jun 9, 2003).
2. B. Derijard *et al.*, *Cell* **76**, 1025 (Mar 25, 1994).
3. H. Yoshizaki *et al.*, *J Cell Biol* **162**, 223 (Jul 21, 2003).
4. O. A. Coso *et al.*, *Cell* **81**, 1137 (Jun 30, 1995).
5. P. Crespo *et al.*, *Oncogene* **13**, 455 (Aug 1, 1996).
6. A. Minden, A. Lin, F. X. Claret, A. Abo, M. Karin, *Cell* **81**, 1147 (Jun 30, 1995).
7. W. G. Kaelin, Jr., *Methods Enzymol* **435**, 371 (2007).
8. B. Bodenmiller *et al.*, *Mol Biosyst* **3**, 275 (Apr, 2007).
9. R. Linding *et al.*, *Cell* **129**, 1415 (Jun 29, 2007).
10. R. Linding *et al.*, *Nucleic Acids Res* **36**, D695 (Jan, 2008).
11. M. Miller *et al.*, *Science Signaling*, (Accepted).
12. P. Shannon *et al.*, *Genome Res* **13**, 2498 (Nov, 2003).
13. V. M. Draviam *et al.*, *Nat Cell Biol* **9**, 556 (May, 2007).
14. K. Oktay, E. Buyuk, O. Oktem, M. Oktay, F. G. Giancotti, *Cell Cycle* **7**, 533 (Feb, 2008).
15. K. Lee, K. Song, *Cell Cycle* **7**, 216 (Jan, 2008).
16. Y. Fan *et al.*, *Biochem Biophys Res Commun* **355**, 263 (Mar 30, 2007).
17. C. Kuntzen *et al.*, *Cancer Res* **65**, 6780 (Aug 1, 2005).
18. R. F. Schwabe *et al.*, *Hepatology* **37**, 824 (Apr, 2003).
19. K. A. Janes *et al.*, *Science* **310**, 1646 (Dec 9, 2005).
20. L. Ciapponi, D. B. Jackson, M. Mlodzik, D. Bohmann, *Genes Dev* **15**, 1540 (Jun 15, 2001).

fig s1

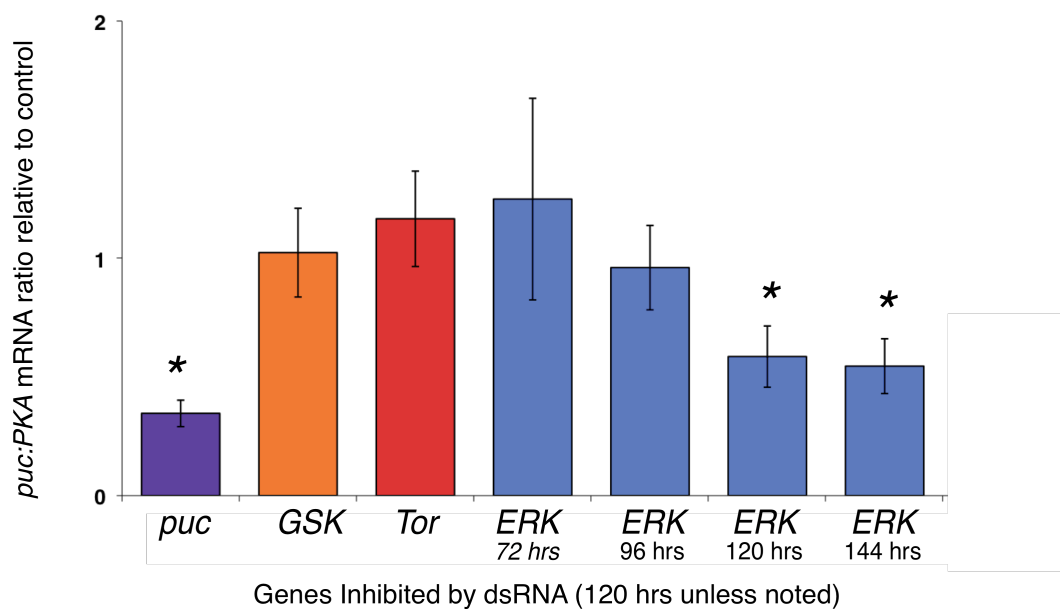


Figure S1. *Puckered* is a transcriptional target of ERK signaling. dsRNAs targeting *ERK* results in significant (denoted by asterisk) decreases as judged by Student's T-test ($P < 0.01$) in *puckered* RNA levels judged by Student's T-test ($P < 0.01$) are denoted by "#".

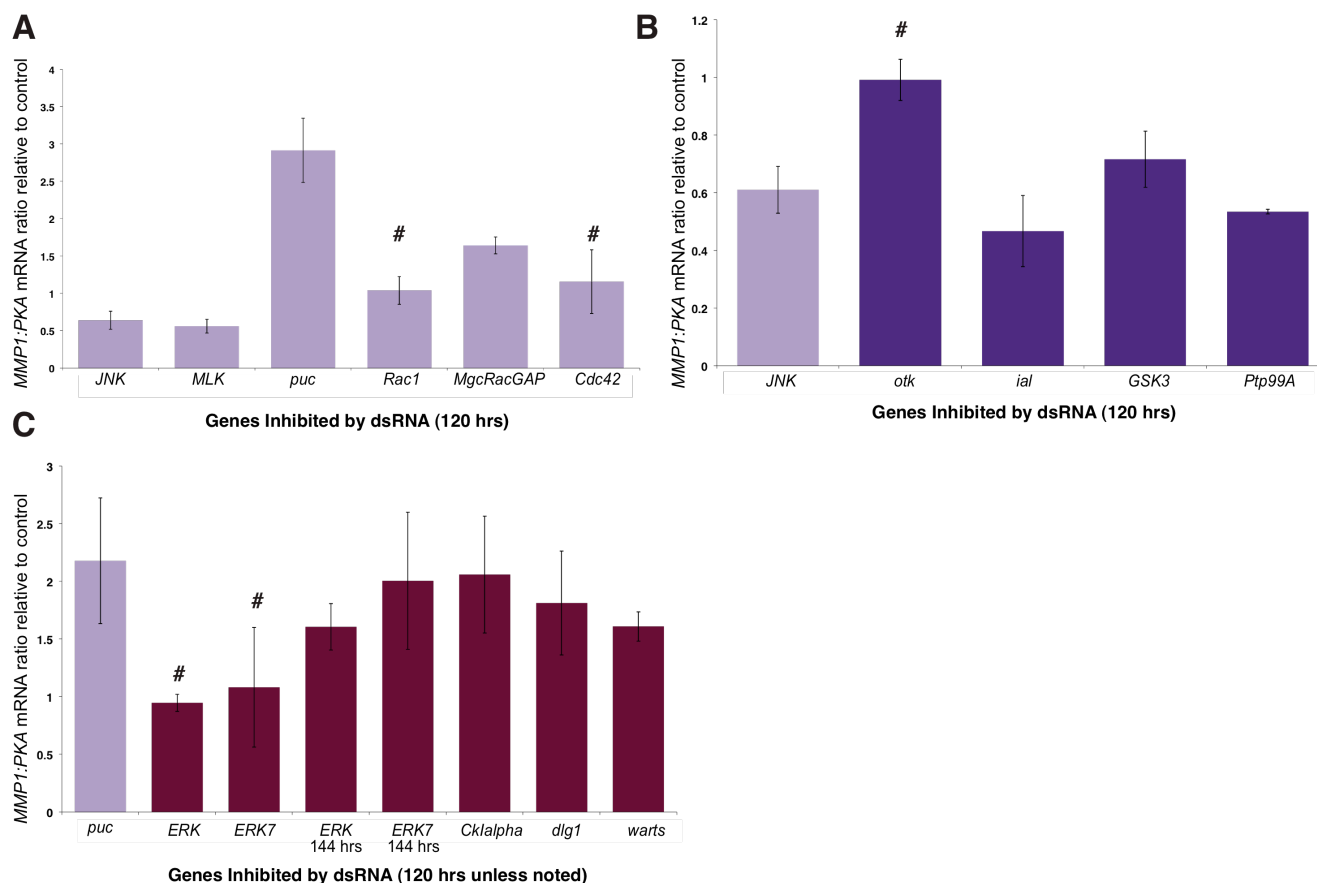


Figure S2. Validation of candidate JNK regulators by monitoring of *MMP1* levels. Quantitative real-time PCR was used to measure mRNA abundance of the JNK transcriptional target *MMP1* following RNAi-mediated inhibition of canonical JNK regulators and *MgcRacGAP*. (A), candidate JNK suppressors (B), or candidate JNK enhancers (C). *MMP1* mRNA levels not significantly different from control cells as judged by Student's T-test ($P < 0.01$) are denoted by "#". *MMP1* levels were observed to significantly rise following inhibition of *ERK* or *ERK7* only after 144 hrs of RNAi suggesting that regulation of *MMP1* levels occurs indirectly through downregulation of *puc* (see fig. s3) and subsequent upregulation of JNK activity.